Journal of Molecular Structure 1084 (2015) 165–171

Contents lists available at ScienceDirect

Journal of Molecular Structure

journal homepage: www.elsevier.com/locate/molstruc

Spectroscopic studies and density functional theory investigations of a cobalt phthalocyanine derivative

Roberto Salcedo [a,*], Liliana Pérez-Manríquez [a], M.E. Sánchez-Vergara [b,*]

[a] Instituto de Investigaciones en Materiales, UNAM, Circuito exterior s/n, Ciudad Universitaria, Coyoacán 04510, México DF, Mexico
[b] Universidad Anáhuac México Norte. Avenida Universidad Anáhuac 46, Col. Lomas Anáhuac, 52786 Huixquilucan, Estado de México, Mexico

HIGHLIGHTS

- The α and β phases of a cobalt derivative have been studied by spectroscopic methods.
- Its complex structure arises from the presence of crystalline and molecular phases.
- Theoretical calculations predict novel deformations on the bond Co-anthraquinone.

ARTICLE INFO

Article history:
Received 25 September 2014
Received in revised form 13 November 2014
Accepted 29 November 2014
Available online 12 December 2014

Keywords:
Phthalocyanine
DFT calculations
Optical properties

ABSTRACT

Colloidal solutions at room temperature were used to obtain various polymorphic forms of a $[PcCoCN]_n$ and double potassium salt from 1,8 dihydroxyanthraquinone derivative. Nanocrystals in the form α and β were characterized using IR and UV–Vis spectroscopy techniques. Likewise in this context, an energy doublet in the absorption spectra of the monoclinic form at 1.8 and 2 eV was observed. The complex structure inherent to the spectra of the CoPc derivative is attributed to the simultaneous presence of both crystalline and molecular phases in the samples. The optical absorption of the compound was also investigated in order to evaluate changes in the electronic structure of these metal organic nanostructures. The absorption spectra of the CoPc derivative recorded in the UV–Vis region manifested two absorption bands, namely the Q- and B- bands. DFT calculations of this structure help to establish the source of the spectroscopic behavior and also lead to a particular phenomenon not known previously in this kind of complex, because the optimized structure of the cobalt complex manifests a very strange deformation of the bond between the anthraquinone derivative and the cobalt atom; the origin of this deformation is also discussed.

Introduction

Phthalocyanine (Pc) is a porphyrin derivative, characterized by high symmetry, planarity and electron delocalization [1]. Pc and their metallic derivatives are currently one of the most important organic compounds due to their ultrafast response times, ease processing and large optical non linearities [2,3]. Metallophthalocyanines (MPcs) show very intense optical absorption values in the visible region. Thus, they are considered likely candidates for optical amplification in the 600–700-nm region, which makes them potentially useful for nonlinear optical applications [4]. Pc and its numerous metallic complexes have been widely used because of their wide-spread applications in the field of solid state technology [5], e.g., optoelectronics, organic nanophotonics and photocopier industry [5–7].

MPcs are plane aromatic macrocycles that constitute four isoindol units joined at their 1 and 3 positions by nitrogen atoms. Their structure consists of 42 π electrons, which extend over 32 carbon atoms and 8 nitrogen atoms. However, electronic delocalization takes place mainly over the inner ring system, in such a way that the phthalocyanine is formally considered as an aromatic system made up of 16 atoms and 18 π electrons. As the central cavity of the phthalocyanine molecule contains hydrogen atoms, these can be replaced by more than 70 different atomic elements, giving them great versatility. MPcs are unique two-dimensional π-conjugated macrocyclic materials, which offer numerous possibilities for molecular engineering and show very effective thermal and chemical stability [5]. Likewise, the Pcs are arranged in crystalline formations, depending on the stacking order of the aromatic rings. Due to the force of the π bonds, they can be accommodated in different structures; this also depends on the substitutes they have. The main crystalline formations of Pcs are alpha (α) and beta (β) [8]. The difference between these

* Corresponding authors.

http://dx.doi.org/10.1016/j.molstruc.2014.11.071
0022-2860/

two types refers to the angle that exists between the symmetry axis and the stacking direction (see Fig. 1 for CuPc). Alpha crystals have a 26.5° angle, while beta crystals have a 45.8° angle. Nanocrystals have been synthesized in a supersaturated solution of a Pc containing a crystallizing liquid that does not dissolve the Pc [2,3]. Akimov et al. [7,9] have obtained MgPc nanocrystals after adding some water to a saturated solution of MgPc in acetone. Rangel-Rojo et al. [10] have pioneered fabrication of Pc nanocrystals from vanadyl-phthalocyanines. MPcs are characterized by polymorphism, as they contain molecular, dimeric and more aggregated associates with either crystalline or amorphous phases [9]. The absorption spectra of different polymorphs from certain phthalocyanine compounds manifest significant differences between them [8,11]. The type of crystallization determines their physical properties.

In this study, we analyze and compare the optical absorption spectra of different aggregate forms of cobalt(II) phthalocyanine derivative $C_{47}H_{22}N_9O_4KCo$, in the simple and binary mixtures of solvents. The first component of the mixture must dissolve the cobalt compound and must provide a solution that is close to saturation. The other components were chosen for not dissolving the MPc derivative, but could be mixed with the first solvent. Diffraction (XRD) was carried out over the compound to search for crystallinity. We also report the important optical parameters related to the principal optical transitions in the UV–Vis region, as well as the surface properties studied by scanning electron microscopy (SEM) and transmission electron microscopy (HRTEM), furthermore DFT calculations were carried out in order to discover the origin of the spectroscopic particularities, however they also provide a very interesting feature concerning the bonding of one of the substituents.

Experimental details

Cobalt (II) phthalocyanine derivative ($C_{47}H_{22}N_9O_4KCo$) was obtained using the procedure reported previously [12] by adding the bidentate ligand: double potassium salt from 1,8 dihydroxianthraquinone ($C_{14}H_6O_4K_2$) to the complex (μ-cyano)(phthalocyaninate)Co(III) or $[PcCoCN]_n$. Initially the solubility of these compounds was evaluated in various polar and nonpolar solvents. Fig. 2 shows the molecular structure for cobalt phthalocyanine derivative.

Add 0.11 g (0.19 mmol) of (μ-cyano)(phthalocyaninato)cobalt(III), $[PcCoCN]_n$ to 0.22 g (0.7 mmol) of double potassium salt from 1,8 dihydroxianthraquinone and dissolve it in 20 ml of methanol (pH = 6). The resulting mixture was maintained under reflux for about 3 days until a precipitate was obtained. Next, the product was filtered, washed with absolute methanol and then vacuum-dried. The product was purified from 1:1 methanol–water. The resulting purple powder was dried under high vacum. IR (KBr, cm^{-1}) ν_{max}: 1615 (C—H); 1508 (C—C); 1123 (C=N); 1083 (C—O); 2152 (CN) [12].

$C_{47}H_{22}N_9O_4KCo$ nanoparticles were prepared in colloidal solutions. According to Akinov et al. [7,9], the first component of the mixture must dissolve the CoPc derivative in a molecular form, whereas the second component is chosen because it does not dissolve the compounds but can be mixed with the first solvent in arbitrary proportions. The addition of the second component to the saturated molecular solution of $C_{47}H_{22}N_9O_4KCo$ has two consequences: simple dilution of the solution and reduction of the limiting solubility of the compound, to the point where the solution reaches supersaturation and the compound precipitates. The solubility of CoPc was evaluated and the following solvents were chosen: acetone, diethylamine and chloroform, which maximize the

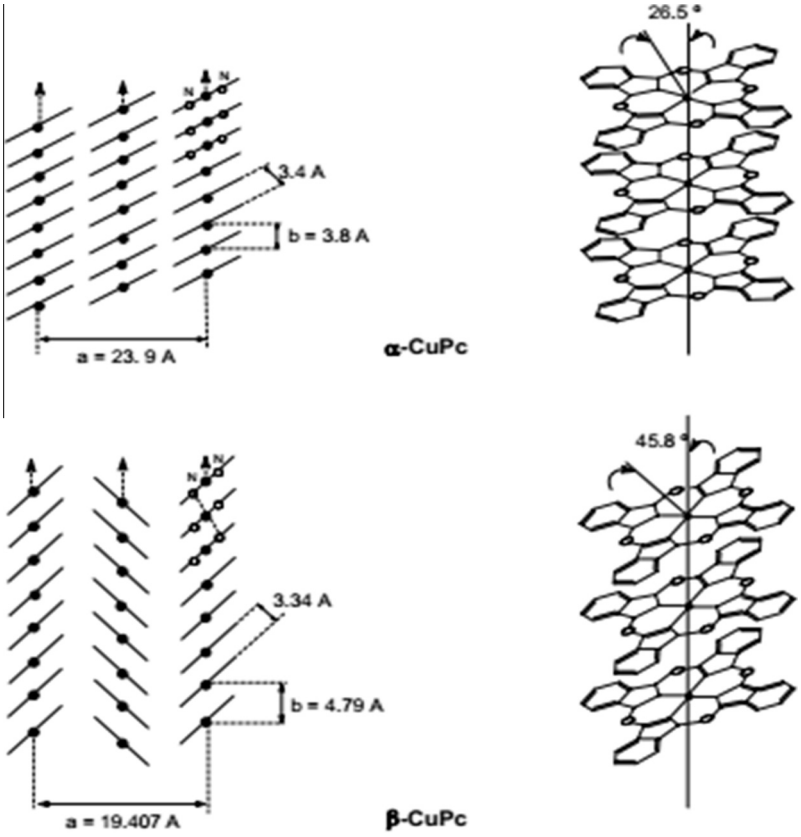

Fig. 1. Crystalline formations of CuPc: alpha (α) and beta (β).

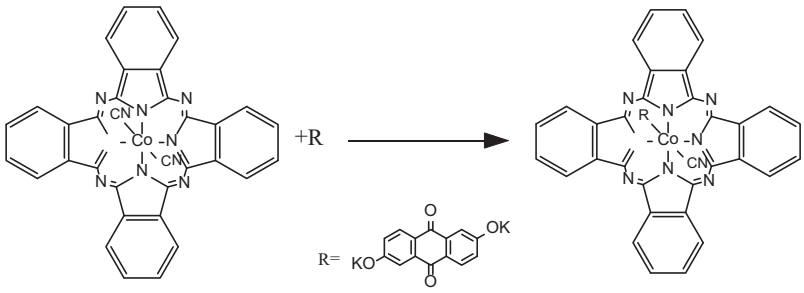

Fig. 2. Chemical structure of the synthesized molecular material obtained from $[PcCoCN]_n$ (R represents the bidentate double potassium salt).

solubility of the dye to about 1 g/L. The second solvent was hexane, where the solubility of the CoPc derivative is less than 10^{-8} g/L. Samples were characterized by FT-IR measurements (Nicolet iS5-FT spectrophotometer), Ultraviolet–visible spectroscopy (*Unicam* spectrophotometer model *UV300*), SEM (*Leica Cambridge* scanning electron microscope model *Stereoscan 440* was coupled to a microanalysis system and operated at a voltage of 20 kV and a focal distance of 25 mm) and HRTEM (High resolution transmission electron microscope JEOL-2010FEG working at 200 kV, fitted with an energy dispersive X-ray spectrometer Noran, Voyager 4.2.3). For the TEM analysis, samples were sonicated in isopropanol for 30 min and then a drop of solution was place on a copper TEM grid for the analysis. Ultrasound is used to separate particles as nano state that usually have the tendency to aggregate. Isopropanol is a solvent only. Upon evaporation, the nanoparticles are dispersed into the grid to differentiate well in the TEM. The X-ray diffraction analysis was performed with the θ–2θ technique using a Bragg–Brentano Rigaku ULTIMA-IV diffractometer and working with Cu K-α (λ = 0.15405 nm) radiation.

Computational methods

All structures were optimized in the gas phase using the Gaussian09 package [13]. In this work, the M06 density functional [14,15] and the 6–31 g** basis set were employed. The frequency calculations were carried out at the same level of theory in order to confirm that the optimized structures were at the minimum of the potential surface. Gaussian 09 time dependent calculations were carried out in order to get the UV–visible theoretical spectrum, the same method and basis set as the optimization calculations were used in this case.

Results and discussion

The purpose of the IR spectroscopic studies on this compound was to identify the most important and representative bonds of the same phase (see experimental details). From these studies we were able to determine any significant chemical change which occurred in these materials during the dissolution procedure. Due to the stability of this compound, chemical changes or reactions are not expected to occur. After adding some hexane to a saturated solution of $C_{47}H_{22}N_9O_4KCo$ in acetone, chloroform or diethylamine, a colloidal solution was formed. IR spectroscopy was used to identify the crystalline nature of the nanocrystals, as the IR spectrum is strongly dependent on the chemical composition and the crystalline form [3,16]. Fig. 3 shows the infrared absorption spectra of CoPc derivative after crystallization in chloroform (1a), diethylamine (1b) and acetone (1c). MPcs are known to have different polyforms, which can be clearly identified using the IR absorption technique [9,16]. The IR bands of the MPcs in the 700–800 cm^{-1} region of the spectra are often used to identify different polymorphs (α, β) because of their sensitivity to the crystal packing arrangement [3,17]. These spectral differences are attributed to the different crystalline stacking of the MPcs molecules, especially those around 731 and 777 cm^{-1} for the β-form and those around 720 cm^{-1} for the α-form, depending on the metal in the Pc and by the modification of its periphery with suitable functional/non-functional groups [8,18]. The peaks in the 750–600 cm^{-1} interval probably result from vibrations in the benzene ring interacting with the pyrrole ring [18], this feature can be demonstrated by the comparison of this spectra with the theoretical one which is shown in Fig. 3d, in this the main signals corresponds to the anthraquinone substituent (all peaks around the interval 1500–1200), but it is possible to appreciate the coincidence of the cluster around 800–600 in which the bending and scissoring movements of the benzene-pyrrole units are focused, near this region there are a cluster with several peaks around the 850–800 cm^{-1} interval, this peaks corresponds to the Co—O bond and they were mentioned after. It should be noticed that the signal at approximately 755 cm^{-1} is related to the non-planar C—H bond vibration [15,19]. In the case of the $C_{47}H_{22}N_9O_4KCo$, the spectrum presents values around 732 and 772 cm^{-1}. From these results, it is possible that the β structure is present, as is the α structure assigned to the 722 cm^{-1}. These results indicate that the CoPc derivative has polycrystalline forms. The difference in the bands intensity is related to the solvent polarity and its interaction with the compound.

In contrast, Fig. 4a shows the absorption spectra of $C_{47}H_{22}N_9O_4KCo$ solutions in acetone, diethylamine and chloroform with hexane at a 1:1 ratio. The invariance of the shape of the absorption spectrum of MPcs in different solvents can serve as a distinct indication of the lack of aggregation in the molecular solution [9]; however in this case, the spectrum changes depend on the type of solvent. In diethylamine, the CoPc derivative spectra contain a single small band with maxima at 597 nm and a broad long-wavelength band at 659 nm. In chloroform, the two bands are small with maxima's at 621 and 666 nm. Total suppression of the band is observed when acetone is added. In this case, adding chloroform or acetone to the solution, promoted conditions for the aggregation of molecules. As a result, aggregates in the suspended state grew, forming colloidal dispersions [9]. Initially, solutions were clear, but as the particles grew, opalescence appeared. Simultaneously, large particles precipitated and grew on the walls or bottom of the beaker, reducing the color intensity of the dispersion. The changes of the absorption spectra in the 550–750 nm region thus reflect the presence of aggregates in several forms: the amorphous α and the crystalline β [9]. These results are similar to those obtained by Akimov et al. [9] for MgPc. In order to investigate the relationship between the aggregation state and the optical absorption and electronic structure of the $C_{47}H_{22}N_9O_4KCo$ solution, the absorbance spectra were plotted in terms of photon energy. This plot is shown in Fig. 4b. The UV–vis optical spectra were analyzed in the absorption region between 1 and 4.5 eV. The absorption spectrum of the monoclinic structure (α-form) has a signal

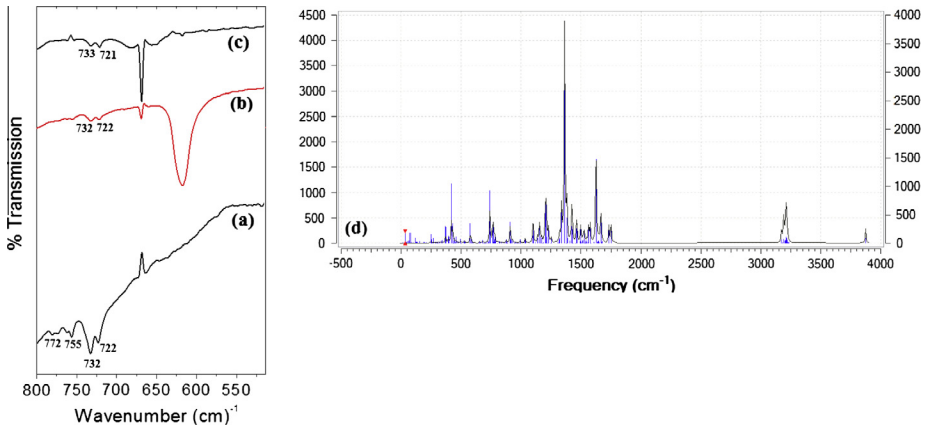

Fig. 3. IR spectroscopies obtained for $C_{47}H_{22}N_9O_4KCo$ in (a) chloroform, (b) diethylamine, (c) acetone and (d) theoretical.

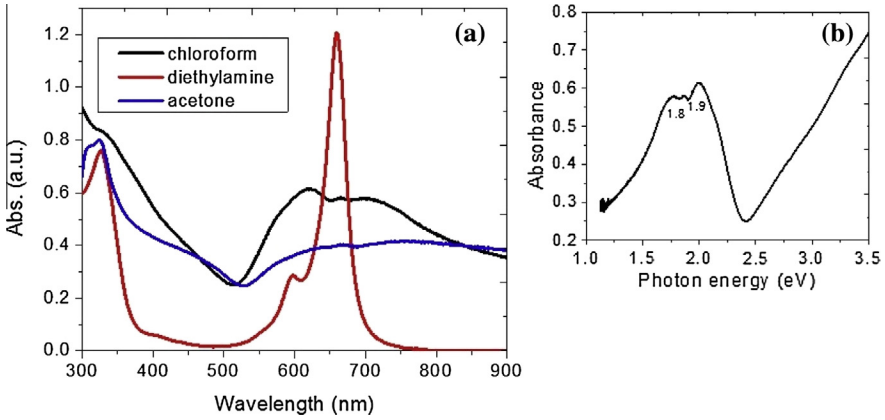

Fig. 4. (a) UV–Vis spectroscopy and (b) Absorbance versus photon energy of $C_{47}H_{22}N_9O_4KCo$.

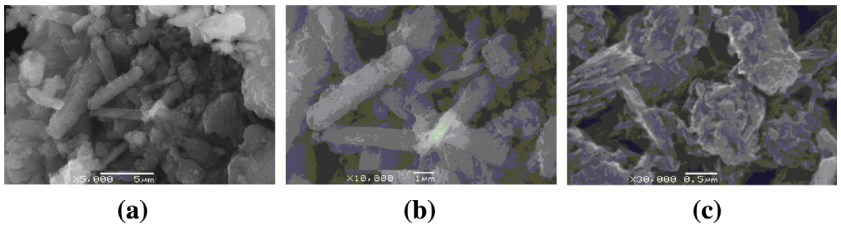

Fig. 5. SEM micrographs of $C_{47}H_{22}N_9O_4KCo$ nanoparticles at (a) 5000×, (b) 10,000× and (c) 30,000×.

around 1.75, whereas the tricyclic spectrum of the (β-form) exhibits a high intensity band at 2 eV [20,21]. The absorption spectrum for CoPc derivative, shows traces of the α phase in the case of the band at 1.8 eV and likewise at 1.9 eV, which may be due to the β phase.

The $C_{47}H_{22}N_9O_4KCo$ aggregates obtained from solution where hexane solvent had been added produced microcrystals at the interface of both solvents. Apparently, the crystallization process takes place in two stages: the first consists of crystal nucleation, and the second corresponds to the growth of the crystal. The driving potential for both stages is the oversaturation. Fig. 5 shows the images obtained by SEM. CoPc derivative manifests conglomerates with irregular shapes and sizes; between 5 μm and 0.5 μm. The texture of the aggregates and their color, clearly indicate a homogeneous composition, in both cases. On the other hand, in Fig. 5, the $C_{47}H_{22}N_9O_4KCo$ sample shows elongated structures similar to those obtained by Lbova et al. for CuPc, which can indicate the presence of the α phase [11], whereas the compact grains may suggest the presence of the β structure. However, the crystalline habits may change when the CoPc derivative growths in different solvents without modification of the crystal structure. For the purpose of detecting whatever signs of crystalline structures, the characterization by means of X-ray diffraction was undertaken on the $C_{47}H_{22}N_9O_4KCo$ aggregates. Fig. 6 shows an X-ray diffraction trace of the CoPc derivative. As it may be observed, there is only one shallow peak at approximately $2\theta = 25°$ implying amorphous structure and the presence of some degree of crystallinity [8]. All this indicates that, while several phtalocyanines have been reported as crystalline polymorphs [8,18,22], during the crystallization process, the kinetic energy in the molecules does not suffice in order for them to possess a high-enough surface mobility. Therefore, the long-reach order, characteristic of crystals, is not achieved

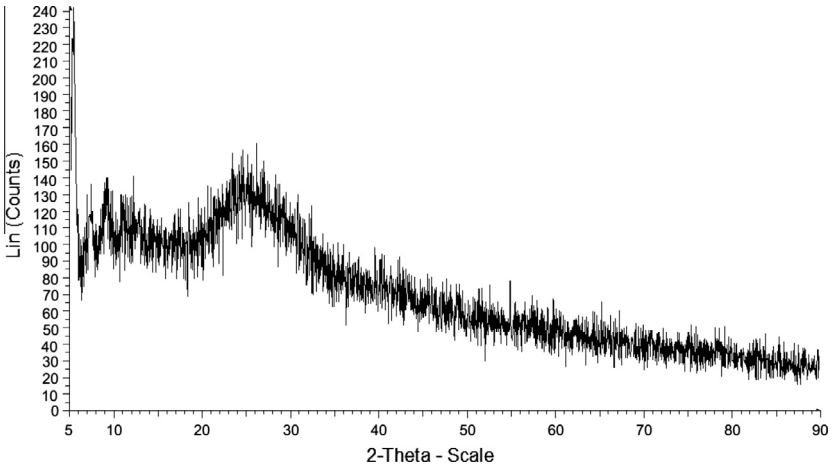

Fig. 6. X-ray diffraction pattern of $C_{47}H_{22}N_9O_4KCo$ nanoparticles.

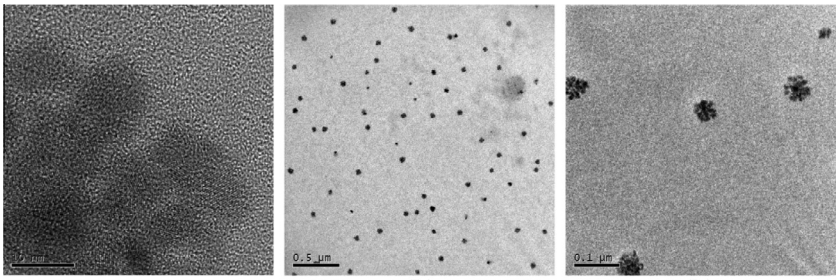

Fig. 7. HRTEM micrographs of $C_{47}H_{22}N_9O_4KCo$ nanoparticles.

and an amorphous structure results. From these results, apparently a mixture of molecular and crystalline forms was obtained for all samples.

By using transmission electron microscopy, a preliminary study of the nanometric CoPcs derivative particles was performed. For instance, Fig. 7 show high resolution images of particles ranging between 0.1 and 10 nm. A heterogeneous dispersion of the nanoparticles can be seen too. From these images, it is also difficult to discern crystalline planes which suggest an amorphous structure. Since the evidence from the IR and UV–vis study show crystalline forms, according X-ray diffraction and TEM, the complex structure of the $C_{47}H_{22}N_9O_4KCo$ is attributed to the simultaneous presence of both crystalline and molecular phases in the MPcs samples.

On the other hand, the UV and visible spectra of the MPcs originates from the molecular orbitals within the 18-π electrons system and from the overlapping orbitals of the central metal atom. The optical absorbance spectra of the MPcs in solution were recorded as ranging between 300 and 900 nm (Fig. 4). Pcs show two typical absorption bands, namely the Q-band in the visible region 530–800 nm and the B-band or Soret band in the violet or near ultraviolet region 300–450 nm [12,20,23]. The Q-band absorption is responsible for the characteristic intense blue/green color of the Pcs [2]. The Q-band have been interpreted in terms of π-π∗ excitation between bonding and anti-bonding molecular orbitals [8]. The electronic spectra of the CoPc derivative show the characteristic Q-band absorption in the 598–713 nm region. However, the Soret-band of the $C_{47}H_{22}N_9O_4KCo$ arising from the deeper π levels →LUMO transitions are observed in the UV region at about 300–339 nm. The Soret band is due to electronic transitions between molecules of an intermediate ionic degree that characterize the synthesized molecular materials. Phthalocyanine derivative absorb light on either side of the blue-green region and may be used as a photoconductor.

Dft calculations

The compound being studied has a somewhat different structure, in the sense that its relatives contain different substituents. In the present case, the phtalocyanine ring is found joined to the central cobalt atom, in the classical tetradentade fashion. The coordination sphere is completed by means of a nitrile ligand in one apex with the functionalized anthraquinone fragment described in the experimental section. The derivative has regular and normal geometry and marked similarities to many other metallic derivatives of this kind [24]. However, if we limit the description to the bonds between the metal atom and the nitrogen terminal points of the ring, the structurally different feature is the bond between the cobalt center and the oxygen atom joined to the anthraquinone derivative. This was expected to have an apical attachment to these ions, but there is a strong deformation where the anthraquinone ligand adopts a position almost parallel in relation to the plane of the ring and the oxygen bond manifests a certain bending which involves even the terminal ring of the anthraquinone fragment, which subsequently is never completely flat; the final geometry is illustrated in Fig. 8.

This distortion is particular to this species and can be explained on the basis of the frontier molecular orbitals, which also manifest different behavior when compared to other complexes from this family. The first curious characteristic is that in spite of any evidence of a clear symmetry point group, both molecular orbitals show very tight twofold degeneration, this indeed is a case of accidental degeneration caused by a possible splitting originated in the

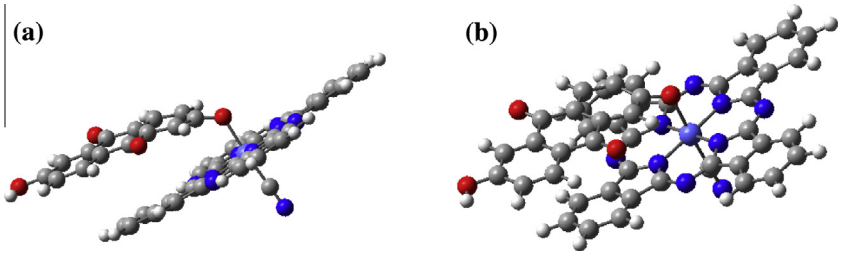

Fig. 8. Two views of the complex (a) the quasi parallel conformation of the anthraquinone fragment is shown; (b) the bond between the oxygen and the cobalt atoms is shown (the code of the colors is the next: Carbon – gray, Oxygen – red, Hydrogen – white, Nitrogen – deep blue, Cobalt – light blue). (For interpretation of the references to color in this figure legend, the reader is referred to the web version of this article.)

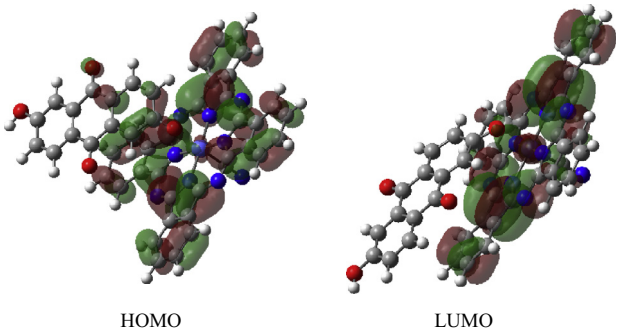

Fig. 9. Frontier molecular orbitals of the molecule under study.

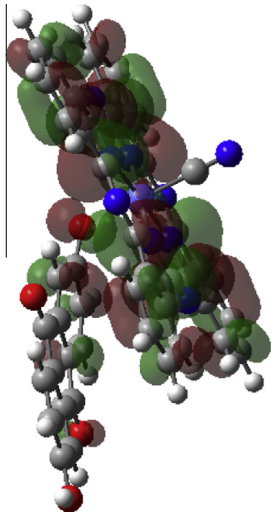

Fig. 10. View of the HOMO showing the interaction between aromatic clouds of the anthraquinone and phtalocyanine fragments.

transition metal center, prior to the apical substitution. The shape of the HOMO and LUMO is shown in Fig. 9.

Both molecular orbitals manifest marked participation on the part of the phtalocyanine fragment, although in the HOMO the wave function also represents an important component derived from the d atomic orbitals of the cobalt, a phenomenon described previously [25]. However the anthraquinone fragment and even the bond between its oxygen terminal atom and the cobalt is only present in the HOMO, indeed in this same orbital this seems to represent some kind of interaction between the aromatic clouds in the tail of the anthraquinone and the aromatic periphery of the phtalocyanine (see Fig. 10), this may therefore be the reason for the unusual arrangement in the anthraquinone moiety, which enables this particular conformation, it is important to mention that the signals (850–800 cm^{-1}) corresponding to the Co—O bond are found in the theoretical spectra as it was outlined above.

The electronic facet is also important; this topic has been the object of multiple studies because this kind of compound can have electronic activity, which makes it suitable for inclusion in research aiming towards the development of devices [26]. The nature of the HOMO and LUMO can change depending on the particular metallic atom at the center and also considering the different possible substituents, therefore the energy gap, the nature of the electronic promotions and changes in multiplicity can vary for the different members of the family. In the present case, the energy gap is relatively short, the value is 1.58 eV, suggesting strong semiconductor behavior; however besides this, a time-dependent calculation makes it possible to deduce the electronic promotions which can be compared to the experimental electronic spectrum. Considering only the first three peaks and a ground state $^1A_{1g}$, the results are 1.72, 1.80 and 1.91 eV (the relevant experimental data is 1.8 eV which corresponds to the α phase as it was mentioned above), and all these promotions involve orbitals from HOMO-1 to LUMO.

Conclusions

We have shown that different forms of $C_{47}H_{22}N_9O_4KCo$ can be obtained from colloidal solutions at room temperature, in the form of nanoparticles. From these results, a mixture of molecular and crystalline forms was obtained. One possible explanation for these results suggests that super small particles which have a broken-up surface interact with the liquid ambient medium and grow to produce nanocrystals. IR and UV–vis spectral analysis confirmed that CoPc derivative contains the α and β forms and the corresponding theoretical spectra were compared with these in order to reinforce the argument. In contrast, the absorption spectra showed evidence for the existence of two absorption regions, identified as the Q and B bands. The DFT calculations show that the electronic promotions correspond to the experimental UV–visible spectra data. Furthermore, a particular distortion on the bond between the central cobalt atom and the anthraquinone substituent is achieved, thus the distortion arises from an accidental degeneracy on the frontier molecular orbitals and the interaction of the aromatic clouds related to both systems.

Acknowledgments

M.E. Sánchez-Vergara acknowledges the financial support provided by SEP-CONACYT-México, project number 153751. Roberto Salcedo would like to thank Joaquin Morales, Alberto López and Caín González for technical help.

References

[1] A.B. Djurišić, C.Y. Kwong, T.W. Lau, W.L. Guo, E.H. Li, Z.T. Liu, H.S. Kwok, L.S.M. Lam, W.K. Chan, Opt. Commun. 205 (2002) 155–162.

[2] a) C. Nitschke, S.M. O'Flaherty, M. Kroell, A. Strevens, S. Maier, M.G. Rüther, W.J. Blau, Organic Photonic Mater. Dev. (2003) 4991V;
b) James G. Grote, Toshikuni Kaino, Editors, Proceedings of SPIE. pp. 124–131.

[3] N. Touka, H. Benelmadjat, B. Boudine, O. Halimi, M. Sebais, J. Assoc. Arab Univ. Basic Appl. Sci. 13 (2013) 52–56.

[4] G.A. Kumar, G. Jose, V. Thomas, N.V. Unnikrishnan, V.P.N. Nampoori, Spectrochimica Acta Part A 59 (2003) 1.

[5] H.S. Nalwa, M. Hanack, G. Pawlowski, M.K. Engel, Chem. Phys. 245 (1999) 17–26.

[6] A.V. Ziminov, Yu A. Polevaya, T.A. Jourre, S.M. Ramsh, M.M. Mezdrogina, N.K. Poletaev, Semiconductors 44 (2010) 1070–1073.

[7] I.A. Akimov, A.M. Meshkov, Opt. Spectrosc. 98 (2005) 415–419.

[8] M.M. El-Nahass, A.M. Farag, Abd-El-Rahman, A.A.A. Darwish, Opt. Laser Technol. 37 (2005) 513–523.

[9] I.A. Akimov, I.Yu. Denisyuk, A.M. Meshkov, A.V. Gorelova, J. Opt. Technol. 70 (2) (2003) 67–71.

[10] R. Rangel-Rojo, S. Yamada, H. Matsuda, H. Kasai, Y. Komai, S. Okada, H. Oikawa, H. Nakanischi, Jpn. J. Appl. Phys. 38 (1999) 69–73.

[11] A.K. Lbova, M.P. Vasiliev, E.S. Gutman, Russ. J. Phys. Chem. A 85 (2011) 457–561.

[12] M.E. Sánchez Vergara, I.F. Islas Bernal, M. Rivera, A. Ortiz Rebollo, J.R. Alvarez Bada, Thin Solid Films 515 (2007) 5374–5380.

[13] Gaussian 09, Revision A.01, M.J. Frisch, G.W. Trucks, H.B. Schlegel, G.E. Scuseria, M.A. Robb, J.R. Cheeseman, G. Scalmani, V. Barone, B. Mennucci, G.A. Petersson, H. Nakatsuji, M. Caricato, X. Li, H.P. Hratchian, A.F. Izmaylov, J. Bloino, G. Zheng, J.L. Sonnenberg, M. Hada, M. Ehara, K. Toyota, R. Fukuda, J. Hasegawa, M. Ishida, T. Nakajima, Y. Honda, O. Kitao, H. Nakai, T. Vreven, J.A. Montgomery, Jr., J.E. Peralta, F. Ogliaro, M. Bearpark, J.J. Heyd, E. Brothers, K.N. Kudin, V.N. Staroverov, R. Kobayashi, J. Normand, K. Raghavachari, A. Rendell, J.C. Burant, S.S. Iyengar, J. Tomasi, M. Cossi, N. Rega, J.M. Millam, M. Klene, J.E. Knox, J.B. Cross, V. Bakken, C. Adamo, J. Jaramillo, R. Gomperts, R.E. Stratmann, O. Yazyev, A.J. Austin, R. Cammi, C. Pomelli, J.W. Ochterski, R.L. Martin, K. Morokuma, V.G. Zakrzewski, G.A. Voth, P. Salvador, J.J. Dannenberg, S. Dapprich, A.D. Daniels, O. Farkas, J.B. Foresman, J.V. Ortiz, J. Cioslowski, D.J. Fox, Gaussian Inc, Wallingford CT, 2009.

[14] Y. Zhao, D.G. Truhlar, Theor. Chem. Acc 120 (2008) 215–241.

[15] Y. Zhao, D.G. Truhlar, Theor. Chem. Acc 119 (2008) 525.

[16] M.M. El-Nahass, K.F. Abd-El-Rahman, A.A. Al-Ghamdi, A.M. Asiri, Phys. B 334 (2004) 398–406.

[17] S. Robinet, C. Clarisse, M. Gauneau, M. Salvi, Thin Solid Films 182 (1989) 307–317.

[18] M.M. Hart. Cationic Exchange Reactions Involving Dilithium Phthalocyanine. Thesis for the degree of Master of Science. Wright State University, 2009.

[19] M.M. El-Nahass, K.F. Abd-El-Rahman, A.A.A. Darwish, Mater. Chem. Phys. 92 (2005) 185–189.

[20] M.E. Sánchez Vergara, A. Ortiz Rebollo, J.R. Alvarez Bada, M. Rivera, J. Phys. Chem. Solids 69 (2008) 1–7.

[21] M.E. Sánchez-Vergara, O.G. Morales-Saavedra, F.G. Ontiveros-Barrera, V. Torrez-Zuñiga, R. Ortega-Martínez, A. Ortiz-Rebollo, Mater. Sci. Eng. (B 158) (2009) 98–107.

[22] T. Del Caño, V. Parra, M.L. Rodríguez-Méndez, R.F. Aroca, J.A. De Saja, Appl. Surf. Sci. 246 (2005) 327–333.

[23] K. Tokumaru, J. Porph. Phthalo. 5 (2001) 77.

[24] S.T. Fujiwara, Y. Gushikem, J. Braz. Chem. Soc. 10 (1999) 389–393.

[25] M.-S. Liao, S. Scheiner, J. Chem. Phys. 114 (2001) 9780–9791.

[26] H. Ali, J.E. van Lier, Chem. Rev. 99 (1999) 2379–2450.